

## Stress analysis between tunnel and slope for single as well as multiple tunnel scenarios: a numerical modelling approach

Ragini Krishna Nikumbh<sup>1,\*</sup> and K. Ram Chandar<sup>2</sup>

<sup>1</sup>Department of Civil Engineering, and

<sup>2</sup>Department of Mining Engineering, National Institute of Technology, Surathkal 575 025, India

Nowadays, a wide accessible network requires a combination of tunnels and roads through highly undulating surfaces. This study aims to assess the stress due to surrounding slope on a tunnel using ANSYS software. A circular tunnel with varying distance between the tunnel and slope, and berm width has been used for the analysis. For multiple tunnel cases, distance between the tunnels was also varied for assessing stresses. In this study, maximum and minimum stresses were obtained for a berm width of 4 and 7 m respectively, which showed that stress decreases with an increase in berm width. For multiple tunnels cases, variations in distance between two tunnels provided significant insights in the analysis of stress between the slope and tunnel.

**Keywords:** Berm width, multiple tunnels, numerical analysis, slope, stress distribution.

LONG and narrow underground openings known as tunnels are drilled through mountains, rocks, soils, etc. to cut down the time and energy needed to facilitate transportation using highways and railways, or for other purposes. These openings are confined except at both ends and are mainly affected by factors such as blocky nature of rocks, fault zones, or as in the case of large-diameter tunnels, the stand-up time of softer ground. The analysis of stress around a tunnel gives us significant information regarding the displacement that its periphery might be prone to. Research has been carried out on a sandstone specimen having a circular opening based on biaxial compression test to imitate the failure of an underground excavation<sup>1</sup>. Various researchers have also carried out numerical modelling analysis to assess stress-induced displacements around the walls of an underground opening for checking its stability<sup>2-4</sup>. Due to decline in the availability of physical space and with advancement in the stresses and displacements analysis for an underground space has led to the idea of drilling multiple openings.

When the *in situ* stresses around an excavated region are within permissible limits, it behaves in an elastic manner, similar to shallow openings in relatively competent geomaterials not subjected to high tectonic stresses.

For multiple tunnels construction, important interaction effects such as unacceptable distortions or bending moments in the existing tunnel liner should/must be considered. The nature of these interactions depends significantly on the tunnel spacing, size of the tunnels, liner stiffness, and the method used to drill the tunnels. Interaction between closely spaced tunnels has been studied in the past using a variety of approaches. Computation of stress distribution around an underground opening gives important information about its stability and the existing stresses around the tunnel periphery have always attracted the attention of researchers in rock mechanics.

Earlier studies related to analysis of rock behaviour around tunnels were based on analytical solution of stress distribution in a stressed elastic plate around a circular hole<sup>5</sup>. The general case of biaxial stress field was studied for three different cases<sup>6</sup>: (a) hydrostatic pressure ( $K_0 = 1$ ), where  $K_0$  is the initial stress ratio; (b) case of  $K_0 = \nu/1 - \nu$ , where  $\nu$  is the Poisson's ratio, and (c) in case of no lateral stress. The effect of proximity of boundary on stress concentration under horizontal *in situ* stress was also analysed<sup>7</sup>. A study on discontinuous rock mass as an assembly of quasi-rigid blocks through deformable joints of definite stiffness was first considered by distinct element method<sup>8</sup>.

In Europe, an alternative tunnel-support design was used based on the development of a plastic zone surrounding the tunnel of approximately one tunnel diameter thickness in the rock mass<sup>9</sup>. According to observations collected from a field in Mont Terri, Switzerland containing hardened, over-consolidated clay, the shape and extent of excavated damaged zone around the tunnel periphery were dependent upon the relative orientation between bedding planes and the axis of excavation<sup>10</sup>. According to some studies, the most severe conditions were experienced when excavation was performed in a direction parallel to the bedding plane strike due to the proliferation of delamination mechanisms (e.g. shearing, bending and buckling of layers), in response to the excavation-induced stress redistribution<sup>11,12</sup>. Various examples of premature borehole collapse have been reported in extended reach and horizontal wells in shale formations with pronounced bedding<sup>13-15</sup>. Increased instabilities with unpredictable failure patterns under isotropic material conditions have also been reported due to the low-strength properties of the bedding planes<sup>16</sup>.

A comprehensive knowledge of the manner in which the rock or soil around a tunnel(s) opening deforms elastically due to variations in stress is of key interest for underground engineering problems. In fact, accurate prediction of the field *in situ* stresses and modulus of deformation by back-analysis of tunnel convergence measurements and by the ground reaction curve, is necessary for the design of reliable support elements for tunnels<sup>17,18</sup>. According to some studies, for tunnels constructed in soft ground below water table, the water flow regime also

\*For correspondence. (e-mail: raginikumbh@gmail.com)

needs to be considered for a realistic analytical model<sup>19,20</sup>.

Stresses induced due to weight of overlying strata and horizontal stresses of tectonic origin have been reported to dominate those occurring on the rock at a depth<sup>21</sup>. Studies on rocky strata have shown, that new stresses were induced due to excavation near an existing tunnel, which was attributed to the rearrangement of *in situ* stresses (during excavation)<sup>22</sup>. The existence of geological structures, rock-mass quality and applied boundary conditions in an anisotropy system of rocks has an affect on the induced stresses<sup>23</sup>. A study on the stress distribution around a circular opening established that before an opening is excavated, the underground stress distribution is uniform and the magnitude of vertical stress increases with depth. After excavation, the portion of strata directly above the opening loses its original support, disturbing the original stress equilibrium<sup>24</sup>. Subsequently, abutment pressure will be developed as the load of immediate roof is transferred on both sides of the opening and the roof starts to sag under gravitational force. The opening will fail either due to fracturing or by deforming excessively, when the stress on an underground opening from the surrounding rock exceeds its tolerable strength.

The stress distribution around an opening in competent rocks, can be approximated from either elastic theory (mathematical models) or from measurements on physical models; these stresses will generally be larger than those obtained at corresponding points on the prototype structure. Thus, a design based on modelling results will be on the conservative side<sup>25</sup>. For careful assessment of possible instability and risk, it is important to identify the state of stress and induced deformation around the tunnel, during the design and construction of any underground excavation<sup>16</sup>.

Results from numerical modelling analysis and *in situ* observations conducted on twin tunnels have shown that for some orientations, the interaction between the twin tunnels could largely influence the soil settlement. Thus, a design for twin tunnels requires numerical analysis along with monitoring them during construction<sup>26,27</sup>. Researchers have also conducted several large-scale model tests to assess the ground behaviour around tunnel-crossing zones and the behaviour of tunnels located above newly excavated ones<sup>28</sup>. The interaction between twin tunnels, with particular importance on the optimization of both the relative positions of the twin tunnels and construction, the procedure using finite element program PLAXIS, has also been studied in the past<sup>29</sup>. Limited studies have been done for assessing the twin tunnel-induced ground movement and their interaction with one another using an analytical solution. The added advantage of such research consists of stress analysis besides a slope adjacent to a modelled highway for both single and multiple tunnel scenarios. The novel part of the present study is the widespread assessment of stresses between the tunnel

and slope; this facilitates proper berm width construction as well as present slope failure and collapse of underground openings.

The main objective of this study was to analyse the stress distribution between the slope and tunnel using numerical modelling and by varying (a) berm width, (b) distance between the tunnel and slope, and (c) distance between two tunnels in the case of multiple tunnel scenario.

The finite element method (FEM) is a numerical methodology for solving problems of engineering and mathematical physics. It is a computerized method to understand how a model will react when it is subjected to forces and other physical effects. The simulations were done using static structural module of ANSYS 14.0 Mechanical APDL software, which uses FEM to analyse the design. Tunnel position(s), changes in berm width, distance between tunnel and slope as well as distance between two tunnels were varied to prepare different models, each being analysed for stress distribution between tunnel and slope. The Solid 65 element with the Drucker–Prager model was used to incorporate cohesion, friction angle and dilatancy angle. The Solid 65 element is defined by eight nodes having three degrees of freedom at each node.

Subsequently, nodes representing different layers were defined and connected in a layer-to-layer format using area tool to represent different soil/rock layers. A tunnel was constituted by subtracting a circular area equal to the tunnel diameter from the material layers using the ‘Booleans’ tool. Extrude option has been used to convert the 2D structure to 3D, and material properties were assigned to the generated model. A ‘Quadrilateral’ mesh element was chosen for analysis. For lower mesh size, stress is underestimated, while it is overestimated for a model having a larger mesh. Rigid support was assigned to the base to restrict displacements along all directions; and roller support was assigned to the side and faces to allow displacement along only one axis. The loads incorporated in the model were: (a) gravity load ( $9.81 \text{ m/s}^2$ ) to incorporate self-weight of the model, and (b) 0.8 MPa pressure applied on the berm width to replicate the live load coming from vehicular movements. The stresses induced due to such pressures are prominent and vital in analysing stress in the tunnel system. The model was analysed for large displacements. Small displacement analysis was avoided in this case, as nodes with small areas get stuck in an infinite loop, and consequently increases the computation time.

A 6 m diameter, circular underground opening was made in the model at a depth of 12 m and running through the soil strata over a layer of highly weathered rocks, on a hard rock formation. In this analysis, fault planes or other discontinuities like fractures or joints have not been considered. Table 1 shows the material properties used to design the model, which were taken

**Table 1.** Material properties used in the model for various soil layers<sup>30</sup>

Soil layer and depth (m)	Saturated unit weight (kg/m <sup>3</sup> )	Young's modulus (N/m <sup>2</sup> )	Poisson's ratio	Cohesion (N/m <sup>2</sup> )	Angle of friction (°)	Dilatency angle (°)
Clayey silt (0–3)	19	5e6	0.35	1e3	40	10
Silty sand (3–8)	21	7e6	0.30	1e3	37	15
Highly weathered rock (8–11.50)	24	3e7	0.35	2e6	50	0
Hard rock (11.50 onwards)	27	7e7	0.35	0	0	0

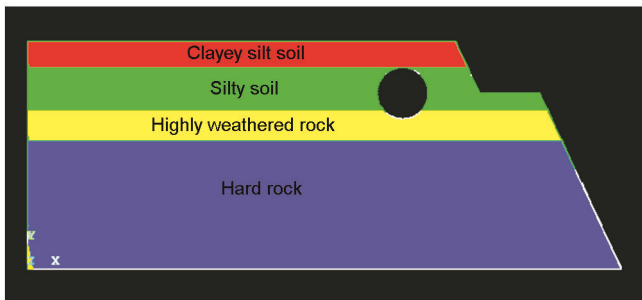


**Figure 1.** Model showing various soil layers for a single tunnel case.

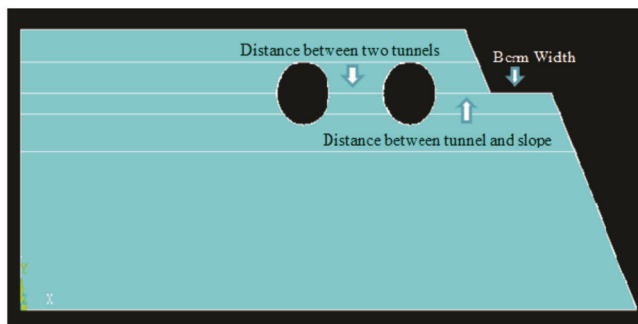


**Figure 2.** Model depicting two excavated tunnels along with berm width.

from an open source<sup>30</sup>. Figure 1 is a pictorial representation of a single tunnel model showing its different soil layers. Variables used in this study are depicted in Figure 2 for multiple tunnels, which are: (a) berm width of 4, 5, 6 and 7 m; (b) distance between tunnel and slope of 3, 4, 5 and 6 m, (c) ratio of distance between the two tunnels to radius of the tunnel of 2, 2.5, 3, 3.5 and 4, i.e. distance between the two tunnels is varied as 6, 7.5, 9, 10.5 and 12 m respectively.

The stress analysis was carried out by varying the berm width and distance between tunnel and slope. In the case of twin tunnels, the distance between the tunnels was also varied and subsequently stress was measured between the tunnel and slope. The maximum horizontal and vertical stresses among all the points computed along the tunnel width were taken into consideration.

For a single tunnel scenario, the vertical stress between tunnel and slope for berm width of 4 and 7 m was 1643.947 and 1391.102 N/m<sup>2</sup> respectively, while the

horizontal stress was 2333.16 and 2095.63 N/m<sup>2</sup> respectively, at 3 m distance between tunnel and slope (Figure 3). The horizontal as well as vertical stresses were found to be lower for the maximum berm width case, i.e. 7 m. The model also showed higher vertical and horizontal stresses when the distance between tunnel and slope was reduced to 3 m for any constant berm width scenario.

Figure 4 shows the maximum horizontal and vertical stress by varying the distance between tunnel and slope for different berm width scenarios. The distance between the two tunnels was kept constant at 6 m. The maximum horizontal and vertical stresses were 2140.81 and 2934.44 N/m<sup>2</sup> respectively, for berm width of 4 m at 3 m distance between the tunnel and slope. The minimum horizontal and vertical stress were obtained for berm width of 7 m, for 6 m distance between tunnel and slope.

Further analysis was carried out for multiple tunnel scenarios, where the distance between two tunnels was varied as 7.5, 9, 10.5 and 12 m. Horizontal and vertical stresses were measured between the tunnel and slope (distance = 3 m) for berm widths of 4 and 7 m (Table 2).

For all the multiple tunnel cases, the maximum horizontal and vertical stresses decreased with increase in berm width. The model depicted higher vertical as well as horizontal stresses when the tunnels were closer to each other, while these stresses decreased with increase in the distance between the two tunnels.

Figure 5 shows the maximum horizontal and vertical stresses by varying berm width and distance between tunnel and slope for 12 m distance between the two tunnels. For berm width of 4 m, the percentage decrease in maximum vertical and horizontal stresses was 18 and 26 respectively, with 3 to 6 m increase in the distance between tunnel and slope. Similar trends of decrease in both vertical as well as horizontal stresses were observed for different berm width scenarios. The above analysis of stresses with variations in berm width and distance between tunnel and slope for single as well as multiple tunnel scenarios provides insight regarding stress distribution around the area between tunnel and slope.

The present study provides important evidences related to stress in both vertical and horizontal directions between tunnel and slope by changing the distance between tunnel and slope as well as berm width. The study demonstrates the following.

(1) For single tunnel models, a maximum stress of 2333.16 and 1643.94 N/m<sup>2</sup> was observed in horizontal

**Table 2.** Maximum horizontal and vertical stresses between the tunnel and slope by varying berm width for multiple tunnels scenarios

Distance between the two tunnels (m)	7.5		9		10.5		12	
Berm width (m)	4	7	4	7	4	7	4	7
Maximum horizontal stress (N/m <sup>2</sup> )	2805.1	2341.98	2774.49	2261.20	2550.39	2169.84	2362.42	1995.11
Maximum vertical stress (N/m <sup>2</sup> )	1978.57	1616.84	1962.44	1638.05	1746.9	1534.27	1757.71	1497.93

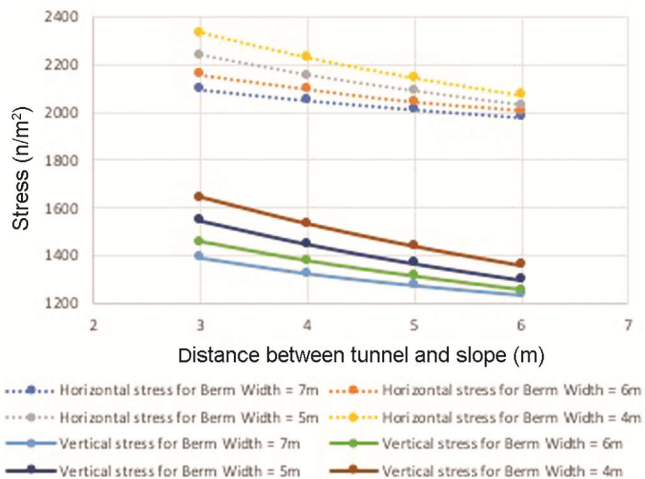


**Figure 3.** The horizontal and vertical stress distribution along the tunnel width for a single tunnel.

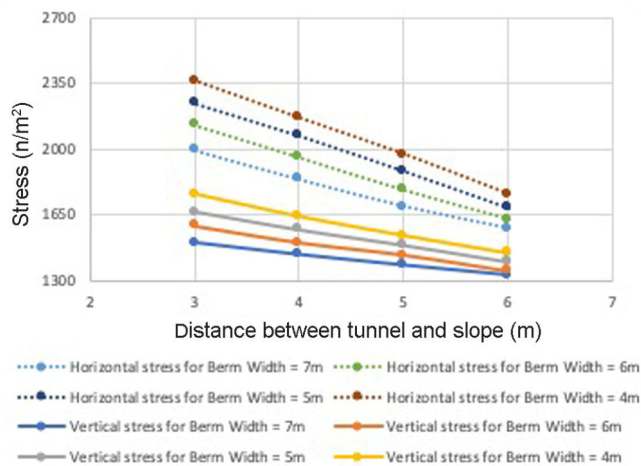


**Figure 5.** Maximum stress (N/m<sup>2</sup>) in the horizontal and vertical direction for different berm widths for multiple tunnels with  $r/a = 4$ .

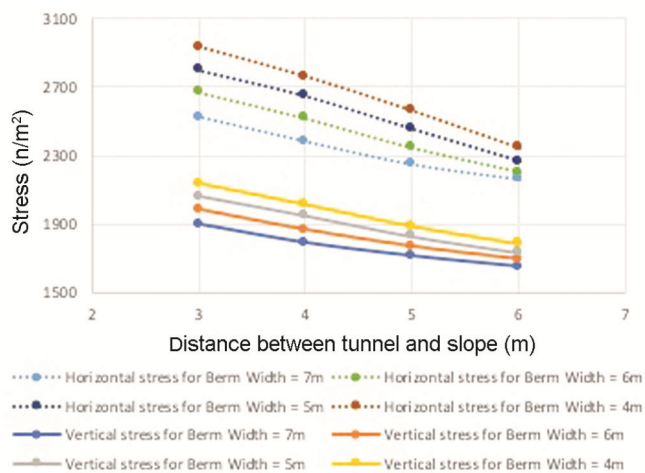


**Figure 4.** Maximum stress (N/m<sup>2</sup>) in the horizontal and vertical direction for different berm widths for multiple tunnels with  $r/a = 2$ .

and vertical directions respectively, for smaller berm width.

(2) For the multiple tunnel scenario with lowest distance between two tunnels, a maximum stress of 2934.44 and 2140.81 N/m<sup>2</sup> is observed between tunnel and slope in horizontal and vertical directions respectively, for berm width of 4 m.

(3) The maximum horizontal and vertical stresses are observed to decrease with increase in the distance between two tunnels, which shows lower magnitude of

stress experienced between the tunnel and slope with greater distance between the two tunnels.

(4) Results indicate that with increase in the distance between the tunnel and slope and keeping the berm width constant, there is decrease in maximum horizontal and vertical stresses. This trend of decrease in stresses in both directions has been observed for both single and multiple tunnel scenarios.

(5) Maximum stress was observed for berm width of 4 m and minimum stress for 7 m. Also, maximum stress in the vertical direction was found to be lower than that obtained in the horizontal direction.

(6) Comparison between single tunnel and twin tunnel scenarios depicts that the maximum horizontal and vertical stresses are observed for twin tunnel in comparison to single tunnel case.

This study on the stress analysis between tunnel and slope for various scenarios provides insights regarding stress distribution for both single as well as multiple tunnel scenarios. The analysis of stresses between tunnel and slope helps us predict the distance at which the tunnel should be placed from the slope without causing slope failure. The assessment of stresses for multiple tunnel scenarios provides an added advantage for proper planning and construction of a new tunnel in the vicinity of an existing tunnel. Such studies will help us to design and

construct safe underground openings as well as provide added safety to nearby structures.

1. Fakhimi, A., Carvalho, F., Ishida, T. and Labuz, J. F., Simulation of failure around a circular opening in rock. *Int. J. Rock Mech. Min. Sci.*, 2002, **39**(4), 507–515.
2. Lee, Y. N., Suh, Y. H., Kim, D. Y. and Nam, H. K., Three-dimensional behavior of large rock caverns. In Proceedings of the 8th International Conference on Rock Mechanics, Tokyo, Japan, 1995, vol. 2, pp. 505–508.
3. Chrissanthakis, P. and Barton, N., Dynamic loading of physical and numerical models of very large underground openings. In Proceedings of the 8th International Conference on Rock Mechanics, Tokyo, Japan, 1995, vol. 3, pp. 1313–1316.
4. Kuili, S. and Sastry, V. R., Prediction and assessment of lateral displacement of rock mass along the length of the Horseshoe Cavern – a numerical modelling approach. *Int. J. Geol. Geotech. Eng.*, 2017, **3**(1), 17–28.
5. Kirsch, G., Die theorie der elastizitat und die bedurfnisse der festigkeit-slehre, *Ver. Deut. Ing.*, 1898, **42**, 797–807.
6. Mindlin, R. D., Stress distribution around a tunnel. *Proc. Am. Soc. Civ. Eng.*, 1939, 619–642.
7. Mindlin, R. D., Stress distribution around a hole near the edge of a plate under tension. *Proc. Soc. Exp. Stress Anal.*, 1948, **2**, 56–68.
8. Cundall, P. A., Explicit finite difference methods in geomechanics. In Numerical Methods in Engineering. Proceedings of the International Conference on Numerical Method in Geomechanics, Blacksburg, 1976, vol. 1, pp. 132–150.
9. Fenner, R., Untersuchungen zur erkenntnis des gerbirgsdruckes, *Gluckuf*, 1938, **74**, 681–695; 705–715.
10. Bossart, P., Meier, P. M., Moeri, A., Trick, T. and Mayor, J. C., Geological and hydraulic characterisation of the excavation disturbed zone in the Opalinus Clay of the Mont Terri Rock Laboratory. *Eng. Geol.*, 2002, **66**(1–2), 19–38.
11. Blumling, P., Bernier, F., Lebon, P. and Martin, C. D., The excavation damaged zone in clay formations time-dependent behaviour and influence on performance assessment. *Phys. Chem. Earth*, 2007, **32**(8–14), 588–599.
12. Marschall, P., Distinguin, M., Shao, H., Bossart, P., Enachescu, C. and Trick, T., Creation and evolution of damage zones around a microtunnel in a claystone formation of the Swiss Jura Mountains, In Proceedings of the International Symposium and Exhibition on Formation Damage Control, Society of Petroleum Engineers, Louisiana, USA, 2006.
13. Gazaniol, D., Forsans, T., Boisson, M. and Piau, J. M., Wellbore failure mechanisms in shales: prediction and prevention. *J. Pet. Technol.*, 1995, **47**(7), 589–595.
14. Oakland, D. and Cook, J., Bedding-related borehole instability in high-angle wells. In Proceedings of the SPE/ISRM Rock Mechanics in Petroleum Engineering, Society of Petroleum Engineers, Trondheim, Norway, 1998.
15. Ong, S. and Roegiers, J. C., Influence of anisotropies in borehole stability. *Int. J. Rock Mech. Min. Sci.*, 1993, **30**(7), 1069–1075.
16. Willson, S. M., Last, N. C., Zoback, M. D. and Moos, D., Drilling in South America: A Wellbore stability approach for complex geologic conditions. In Proceedings of the Latin American and Caribbean Petroleum Engineering Conference, Caracas, Venezuela, 1999; <https://doi.org/10.2118/53940.MS>
17. Hoek, E. and Brown, E. T., *Underground excavations in rock*. Institute of Mining and Metallurgy, London, UK, 1980.
18. Brady, B. H. G. and Brown, E. T., *Rock Mechanics for Underground Mining*, Allen & Unwin, London, UK, 1985.
19. Ferna Àndez, G., Behavior of pressure tunnels and guidelines for liner design. *J. Geotech. Eng. ASCE*, 1994, **120**(10), 1768–1791.
20. Ferna Àndez, G. and Alvarez Jr, T. A., Seepage-induced effective stresses and water pressures around pressure tunnels. *J. Geotech. Eng. ASCE*, 1994, **120**(1), 108–128.
21. Eberhardt, E., *UBC Geological Engineering EOSC*, 2013, p. 433.
22. Raji, M. and Sitharam, T. G., Stress distribution around the tunnel: influence of *in situ* stress and shape of tunnel. In Proceedings of the Indian Geotechnical Conference, Kochi, 2011, p. 290.
23. Joshi, G. R., Numerical simulation of state of stress, deformation and displacement measurements associated with the design of circular tunnel in Himalayan brittle rocks. *GeoMod Portugal*, 2010, 1–5.
24. Peng, S. S. and Chiang, H. S., *Longwall Mining*, Wiley, New York, USA, 2nd edn, p. 708.
25. Arshadnejad, Sh. and Goshtasbi, K., Analysis of the radial and tangential stress distribution between two neighboring circular holes under internal pressure by numerical modelling. *J. S. Afr. Inst. Min. Metall.*, 2011, **111**(5), 301–308.
26. Soliman, E., Duddeck, H. and Ahrens, H., Two- and three-dimensional analysis of closely spaced double-tube tunnels. *Tunnell. Undergr. Space Technol.*, 1993, **8**(1), 13–18.
27. Yamaguchi, I., Yamazaki, I. and Kiritani, K., Study of ground-tunnel interactions of four shield tunnels driven in close proximity, in relation to design and constructions of parallel shield tunnels. *Tunnell. Undergr. Space Technol.*, 1998, **13**(3), 289–304.
28. Byun, G. W., Kim, D. G. and Lee, S. D., Behaviour of the ground in rectangularly crossed area due to tunnel excavation under the existing tunnel. *Tunnell. Undergr. Space Technol.*, 2006, **21**(3–4), 361–367.
29. Chehade, F. H. and Shahrour, I., Numerical analysis of the interaction between twin tunnels: influence of the relative position and construction procedure. *Tunnell. Undergr. Space Technol.*, 2008, **23**, 210–214.
30. Sarika, K., Numerical prediction of vibrations generated by the passage of metro trains in underground tunnels. M Tech thesis, NITK, Surathkal, 2013.

Received 8 October 2018; revised accepted 20 May 2020

doi: 10.18520/cs/v119/i3/551-555